ORIGINAL PAPER

Influence of deep seated discontinuities on the left slope of Jinping I Hydropower Station and its stability analysis

Shengwen Qi · Faquan Wu · Yuande Zhou ·
Yuhuan Song · Manfu Gong

Abstract This paper presents a case history detailing the development of cracks within a rock mass up to 350 m from the steeply incised valley slopes of the Yalong river in South West China, where the Jinping I dam is being constructed. The cracks have opened along previous tectonic structural features such that they penetrate further into the rock mass in the metasandstones and slates than in the marble. The presence of these cracks significantly reduces the stability of the near surface rock mass, requiring major excavation at the dam abutment. Analysis has indicated that the most appropriate way of stabilizing the slopes before the dam is constructed is by grout-infilled, specially constructed galleries which extend 60–80 m from the freshly excavated abutment.

S. Qi (✉) · F. Wu · Y. Song
Key Laboratory of Engineering Geomechanics,
Institute of Geology and Geophysics,
Chinese Academy of Sciences, Beijing 100029, China
e-mail: qishengwen@mail.iggcas.ac.cn

F. Wu
e-mail: wufaquan@mail.iggcas.ac.cn

Y. Song
e-mail: gcdz@mail.iggcas.ac.cn

Y. Zhou
Department of Civil Engineering,
The University of Hong Kong, Pokfulam Road,
Hong Kong, Hong Kong, China
e-mail: yuande@hku.hk

M. Gong
Institute of Chengdu Investigation and Design of National
Electrical Power, Chengdu, Sichuan 610072, China
e-mail: gmanfu@sina.com

Résumé L'article présente une étude de cas détaillant le développement de fissures au sein d'un massif rocheux jusqu'à 350 m à l'intérieur de versants raides, façonnés par la rivière Yalong dans le sud-ouest de la Chine où le barrage de Jinping I est en cours de construction. Les fissures se sont ouvertes le long de discontinuités structurales préexistantes, se propageant au-delà dans des grès métamorphiques, des ardoises et des marbres. La présence de ces fissures réduit de façon significative les conditions de stabilité du massif rocheux près de la surface, nécessitant un approfondissement des excavations pour les fondations du barrage. L'analyse a montré que la façon la plus appropriée pour stabiliser les pentes, avant la construction du barrage, était de procéder à des injections de coulis jusqu'à 60–80 m depuis l'appui rocheux excavé, à partir de galeries spécialement construites.

Introduction

In recent years, due to the huge increase in demand for energy and the need to reduce emissions, China is planning/undertaking a number of hydropower developments, many of which will be at the eastern margin of the Qinghai-Tibetan Plateau where the topography, precipitation and limited population provide ideal sites for hydropower schemes. During construction, some of the slopes have been found to contain fractures deep within the rock mass.

Fig. 1 The topography of the dam site

This paper presents a case study related to these deep seated deformations, with particular emphasis on those found on the left slope of the Jinping I Hydropower Station. It discusses the characteristics of the rock mass and the stability of the hillslopes in the area of the dam.

Geological settings

Topography

Jinping I is located at the west side of a sharp bend in the Yalong River (Wu et al. 2010). The 305 m high double-curvature arch dam will be constructed in a typical V-shaped valley (Fig. 1) where the steep slopes on the left-hand side rise at an angle of 70°–80° below 1,900 m asl, above which they are 40°–50°. The orientation of the valley is N025°. The water level in the river was approximately 1,630 m asl and the reservoir will be impounded to provide a top water level of ca. 1,880 m asl. The mean run-off at the dam site is about 1,200 m³/s.

Lithology

At the dam site the main strata consist of a series of metamorphic rocks of the Zagunao Group of Middle to Upper Triassic age. The spatial distribution of the rocks and faults is shown in Fig. 2 and a cross section in Fig. 3. The lowest member (T_{2-3Z}^1) is a calcareous green schist. The second member (T_{2-3Z}^2) is about 600 m thick and consists of marble, brecciated marble and lenses of cal-careous phyllites and green schist with some layers of crystalline limestone. The third member (T_{2-3Z}^3) is 400 m thick and consists mainly of slates (48%) and metasand-stone (52%).

In addition, as shown in Fig. 2, a lamprophyre dyke is present, striking N060°–080° and dipping towards the SE at an angle of 70°–80°. The dyke is generally 2–3 m wide and is known to extend for some 1,000 m (Fig. 2).

Structures

As shown in Fig. 3, the Jinping I dam site is located approximately 2 km from the Jinping Mountain Fault. The main structures at the dam site are the Santan syncline and four groups of faults which strike NNE, NE, ENE and NW respectively. The major faults which control the slope stability include fault f_5 and fault f_8.

The Santan syncline is an overfolded structure, such that both limbs dip in the same direction. It strikes NNE and can be mapped for a distance of 15 km. As the strike direction of the strata is almost the same as the orientation of the river, the normal limb of the syncline outcrops on the right slope while the inverted limb is located on the left slope (see Fig. 3); hence on the right the strata dip towards the free face but on the left into the mountain mass.

The orientations/declinations of the four sets of discontinuities developed in the left slope are shown in Fig. 4.

(a) Set 1, with an attitude of 285°–350° and a declination of 25°–45° originated as bedding planes. They dip into the slope and strike almost parallel to the river valley. The sandy slates have thin bedding partings (<200 mm) while in the marble the bedding is usually thickly spaced (>400 mm).

(b) Set 2, with an attitude of 90–160° and a declination of 50–80°, has medium to widely spaced joints (0.3–1 m) in the left slope. They are persistent over lengths of 3–5 m with some extending for a length of 10 m. These joints strike almost parallel to the river and dip outwards, towards the free face.

(c) Set 3, with an attitude of 180°–210° (0°–30°) and a declination of 60°–80°, are rarely developed but when present are generally open with no infill.

(d) Set 4, with an attitude of 40°–60° and a declination of 60°–80°, are generally 1–2 m apart and have lengths of 1–3 m, some extending to 3–5 m.

Characteristics of the rock mass and deep seated slope discontinuities

In order to further investigate the deep seated discontinuities and evaluate their effect on the slope stability, a total of 29 exploration adits were excavated at different elevations (Fig. 5a–c).

During these investigations, it was noted that there were well developed cracks up to 300 m into the rock mass from

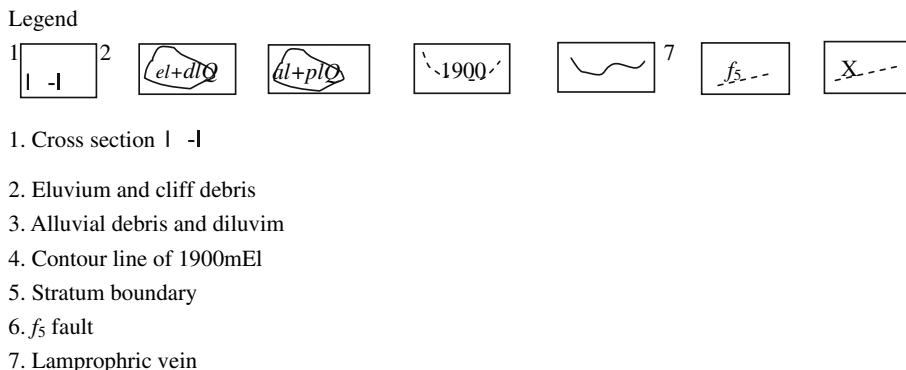**Fig. 2** Geological sketch of the dam site (After Qi et al. 2004)

Legend

1. Cross section Ⅰ -Ⅰ

2. Eluvium and cliff debris
3. Alluvial debris and diluvim
4. Contour line of 1900mEl
5. Stratum boundary
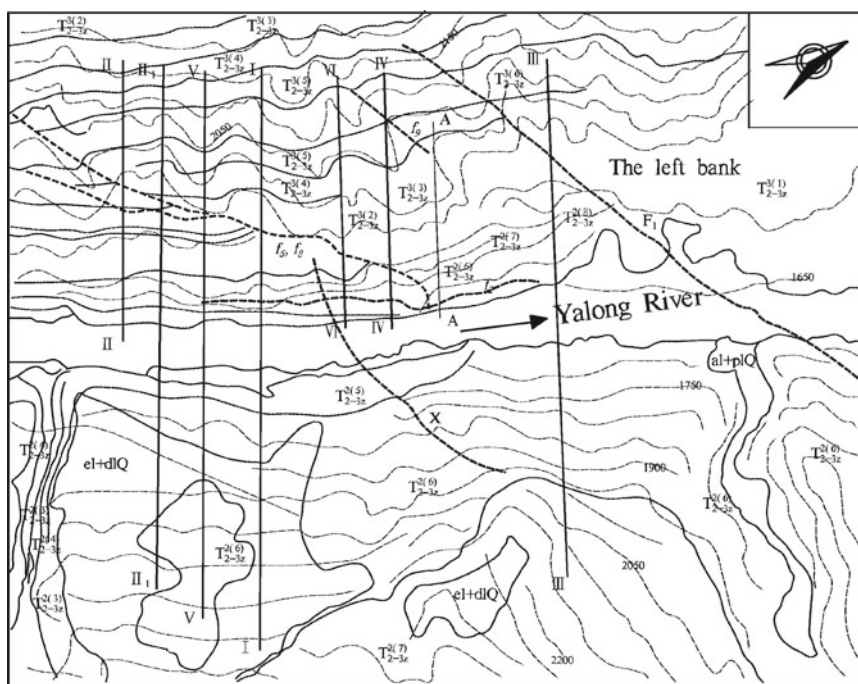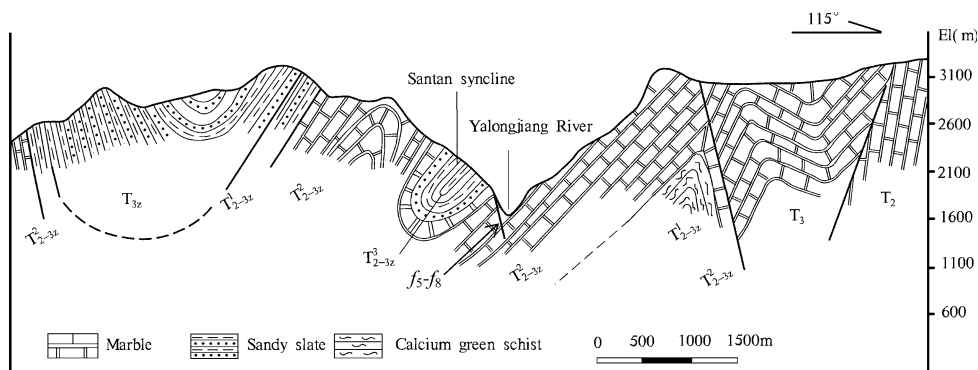6. f_5 fault
7. Lamprophric vein

Fig. 3 Typical geological cross section of the dam site (Along dam axial section of II₁-II₁, see Fig. 2)

the slope face (Fig. 6). Such a distance is much beyond the effect of unloading/de-stressing related to the valley sides; hence they are referred to as "deep cracks". Qi et al. (2004) detailed the distribution of these deep cracks and discussed their formation. In view of their importance, this paper reviews both their distribution and the characteristics of the rocks in which they are found.

Field investigation shows that deep cracks originate as tectonic discontinuities hence their shapes and sizes are limited by the tectonic structures (Qi et al. 2004). In some cases they are open and in others tight, such that they resemble pull-apart structures (Burchfiel and Stewart 1966) where minor deflections mean that once the movement has passed an asperity there will be a gap but downslope of the
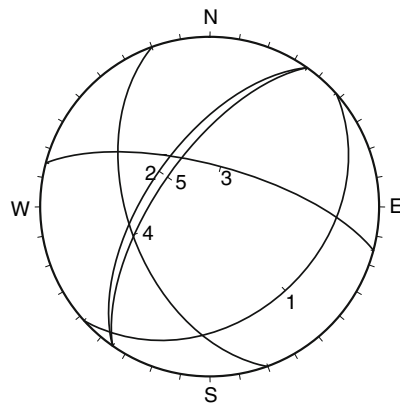
1 — mean attitude of set ①, 318°∠34°;
2 — mean attitude of set ②, 125°∠65°;
3 — mean attitude of set ③, 195°∠70°;
4 — mean attitude of set ④, 70°∠50°;
5 — mean attitude of slope surface, 125°∠60°;

Fig. 4 Stereo net projection of four sets discontinuities and slope surface (Equal area, upper hemisphere)

asperity the rock will be in close contact e.g. SL15 (see Fig. 7a). In some places there are many closely spaced fresh fractures with an aperture of 10–20 mm (e.g. SL3, Fig. 7b), whilst in others there is a single large crack with an aperture of 50–200 mm (e.g. SL14, Fig. 7c). The deep cracks dip outward towards the slope face; the dominant dip direction is N120°–160° at a declination of 50°–60° (similar to the Set 2 joints); a few of the deep cracks have a slightly different attitude with a dip direction of 160°–175° and an angle of 60°–80°.

It has been noted that these deep cracks often have a newly fractured segment where up to 80 mm of downward
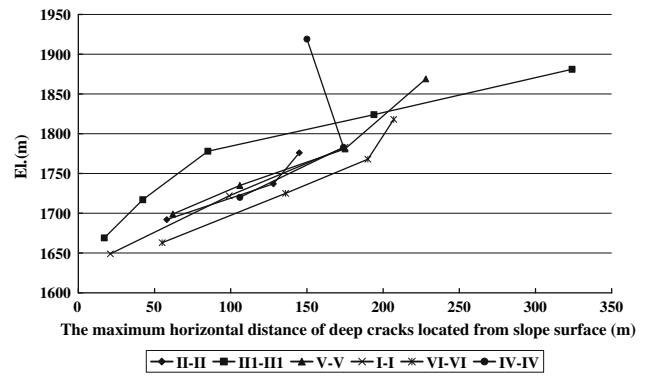

Fig. 6 The maximum horizontal distance of deep cracks located from the slope surface increasing with high elevation

movement appears to have occurred with gravity due to movement in the near surface rocks (e.g. SL24, Fig. 8). Observations in the adits and seismic tomography indicate that the deep cracks extend up to 180 m in their strike direction and up to 60 m in the dip direction. As noted above, the deep cracks are found up to 350 m from the valley side; the horizontal distance increases significantly with elevation (see Fig. 6) with most of the cracks occurring above 1,770 m asl (Qi et al. 2004).

Based on a comprehensive series of tests, the characteristics of the rock mass with deep cracks are summarized as below:

(a)   Statistics show that the discontinuities developed in the rock mass which contained deep cracks were generally fresh and free of filling. The quality of the rock mass is poor with a volumetric joint count (Jv)
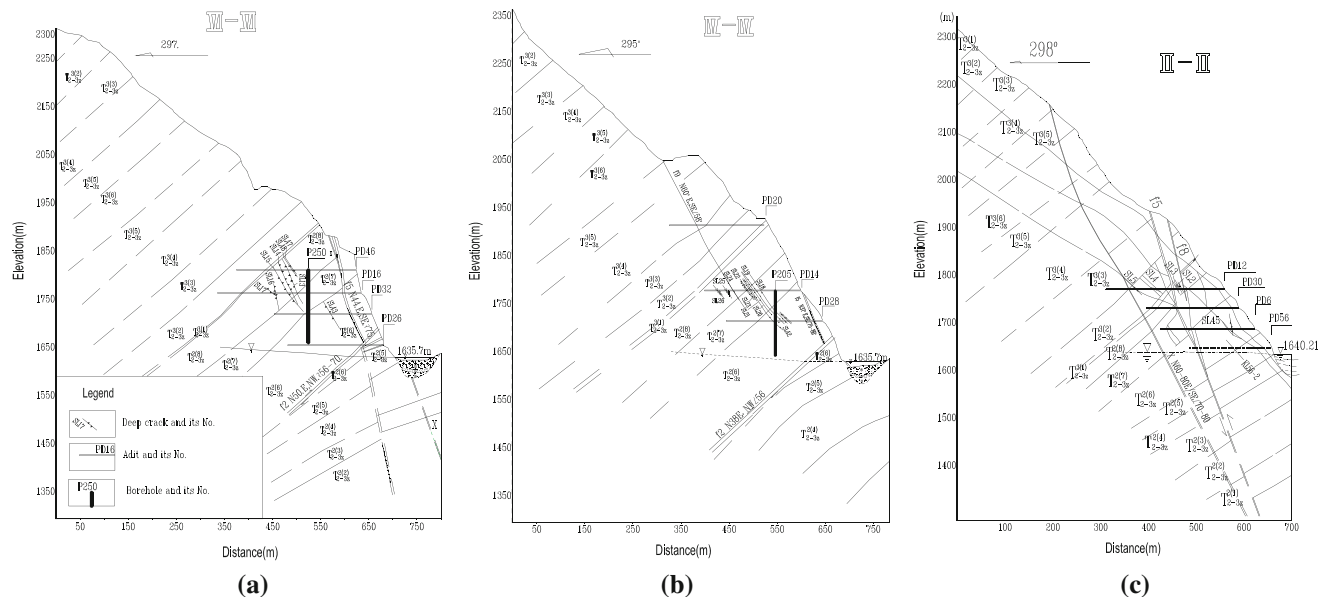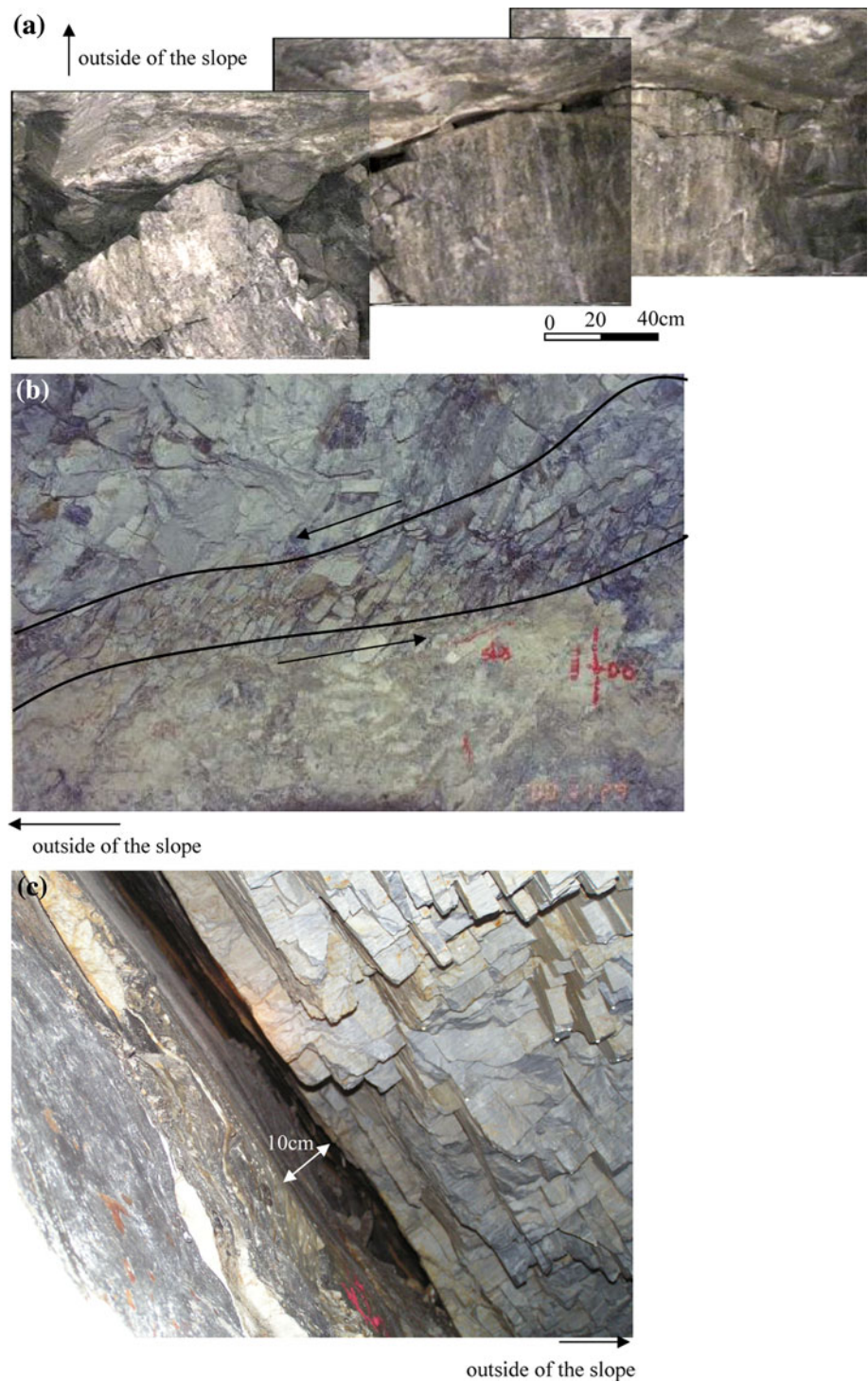

Fig. 5 Typical cross sections of the left bank slope: **a** VI-VI; **b** IV-IV; **c** II-II

Fig. 7 Shape of deep cracks:
a part of deep crack of SL15;
b part of deep crack of SL3;
c part of deep crack of SL14

>20 and an RQD of 25–45. In order to describe the integrity of the rock mass, an index, Kv (integrity coefficient), was adopted in the Chinese Code of Engineering Rock Mass Classification (GB 50218-94). Kv can be obtained by:

$$Kv = \left(V_{pm}/V_{pr}\right)^2 \tag{1}$$

in which V_{pm} is the P wave velocity of the rock mass and V_{pr} it the P wave velocity of the rock block. According to the test results, rock masses with deep
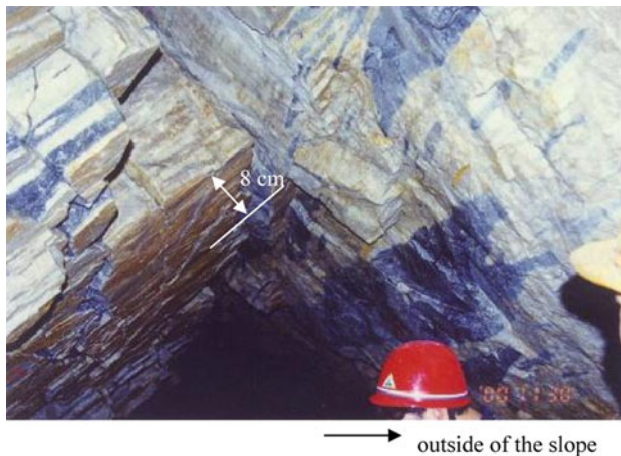
Fig. 8 Deep crack of SL24 with newly fractured segment with downward dislocation (After Qi et al. 2004)
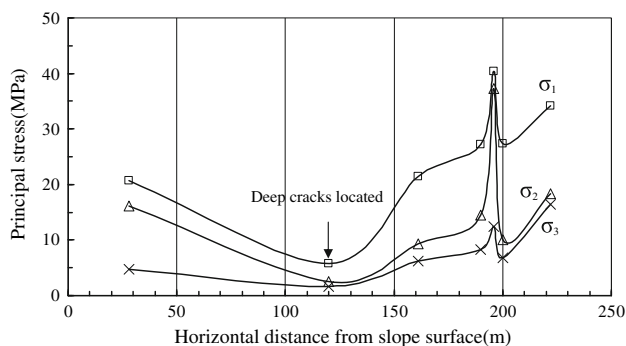

Fig. 9 The distribution of principal ground stress from the slope surface at a horizontal elevation of 1,830 m asl (After Institute of Chengdu Investigation and Design of National Electrical Power 2001)

cracks have a Kv of about 0.08–0.4 and would be assigned to the fractured-extremely fractured rock mass according to the Chinese Code (GB 50218-94).

(b) Hydraulic pressure tests indicate that where deep cracks have developed, the permeability (k) is >100 Lugeons, but in the intact rock between the deep cracks k is <1 Lugeon. Interestingly, the higher permeabilities are present on the left slope, towards the Qinghai-Tibet plateau.

(c) The acoustic wave velocity tests indicate the Vp of the rock mass containing the deep cracks is 1,800–3,500 m/s, i.e much less than that of the rock mass beyond the weakly unloaded zone which is between 3,800 and 4,800 m/s or the rocks well away from the slope where the Vp is >5,500 m/s.

(d) In situ plate loading tests were carried out in SL3 (Fig. 7b), which appeared to be a relatively dilated zone located in adit PD 12 some 99 m from the valley side. This zone contains several small fractures with an accumulated dilation of 30–100 mm. The plate loading test indicated that the deformation modulus parallel to the face of SL3 is 1.2 GPa, and the deformation modulus crossing the face is approx. 0.66 GPa.

(e) Partly owing to the existence of deep cracks in the left bank, the ground stress shows large fluctuations with horizontal distance, increasing inwards from the valley side. For example, at 1,830 m asl (Fig. 9) the ground stress varies with a maximum primary stress of 27.1–40.4 MPa at a distance of 195 m from the slope surface although it drops quite suddenly at 200 m. At a distance of 120–130 m, the ground stress shows an obviously abnormal low magnitude of 5.84 MPa where deep cracks SL14 and SL15 are present. It is possible that the stress concentration at 195 m will form the locus of a future fracture.

Two rock mass classification systems were adopted to evaluate the rock mass with deep cracks:

(a) Geomechanics Classification (RMR) (Bieniawski 1979):

– Intact rock strength, UCS = 80 MPa; Rating = 7;
– Drill core quality, RQD = 25–45%; Rating = 8;
– Spacing of discontinuities, range 55–900 mm; Rating = 5;
– Condition of discontinuities; slickensided surfaces, sometimes with separations >5 mm; Rating = 0–10, average 5;
– Groundwater: Completely dry or damp; Rating = 15–10; average 12.5;

The basic RMR was therefore: 7 + 8+5 + 5+12.5 = 37.5;

The deep cracks strike almost parallel to the valley sides and dip towards the river, hence the "unfavourable" adjustment was made—RMR = 37.5 − 50 = −12.5 indicating a Class V, very poor rock.

(b) Q-system (Barton et al. 1974):

– RQD = 25–45%;
– Jn = 15; four or more random joint sets, heavily jointed;
– Jr = 0.5–1.5; slickensided planar, slickensided undulating;
– Ja = 2.0; slightly altered joint walls, durable mineral coatings, sandy particles, clay-free disintegrated rock, etc.
– Jw = 1.0; dry excavation or minor inflow;
– SRF = 5.0–7.5; multiple shear zones in competent rock (clay-free), loose surrounding rock (any depth);

Table 1 Stability analysis result of cross section of VI-VI and IV-IV with Sarma (1979) method

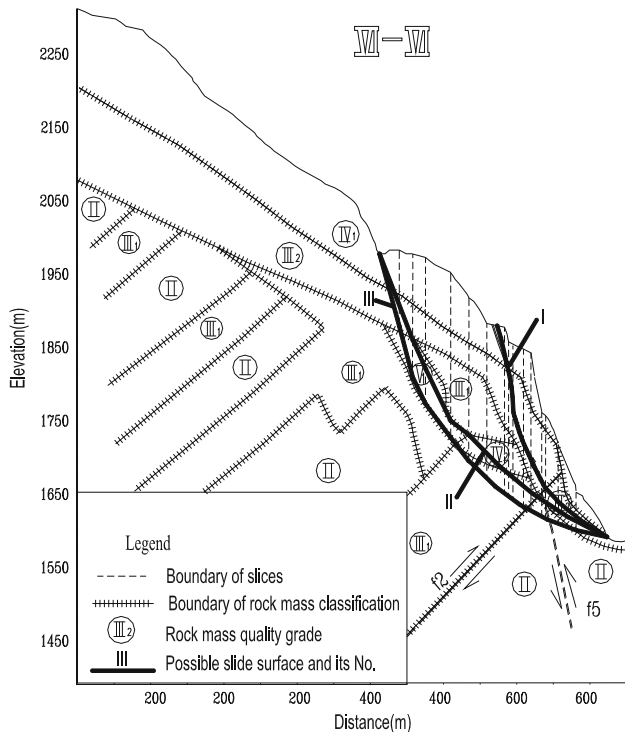| Cross section	No. of critical surface	Possible critical surface	FOS
VI–VI	I	Part of f_5 + speculated segment	1.026
	II	Speculated segment + SL13-14 + speculated segment	1.118
	III	Speculated segment + SL15 + speculated segment	1.300
IV–IV	I	f_9 + SL22-20 + SL42 + speculated segment	1.053
	II	f_9 + SL24 + speculated segment	1.276

Fig. 11 Discretization of IV-IV cross section of the slope

Griffith and Lane's (1999) strength reduction method based on FLAC^{3D} were used to determine the FOS (Factor of Safety) of the slope.

Numerical model

Two typical cross sections (IV-IV and VI-VI) in which deep cracks had developed (Fig. 5a, b) were selected to evaluate the stability of the slope.

From the geological conditions in these cross sections, it is possible to identify a number of likely slide surfaces, as listed in Table 1 (see Figs. 10 and 11) where the rupture plane follows an almost circular line moving from crack to crack, i.e. not typical of a rock slope analysis.

Material parameters

According to the RMR system (Bieniawski 1979), the rock mass of the left slope was classified into four grades: i.e. II–V, with grades III and IV further divided into III$_1$, III$_2$ and IV$_1$, IV$_2$. Based on a number of laboratory and in situ tests, a summary of the mechanical parameters for each grade is given in Table 2, together with the shear strength of the discontinuities.

Fig. 10 Discretization of VI-VI cross section of the slope

This gives a Q value (RQD/Jn × Jr/Ja × Jw/SRF) of = 35/15 × 1.0/2.0 × 1.0/6.75 = 0.173, again representing very poor rock.

Stability analyses

As described above, the characteristics of the rock mass containing deep seated deformations indicate that the deep cracks are likely to weaken the stability of the left bank. The Sarma limited equilibrium approach (Sarma 1979) and
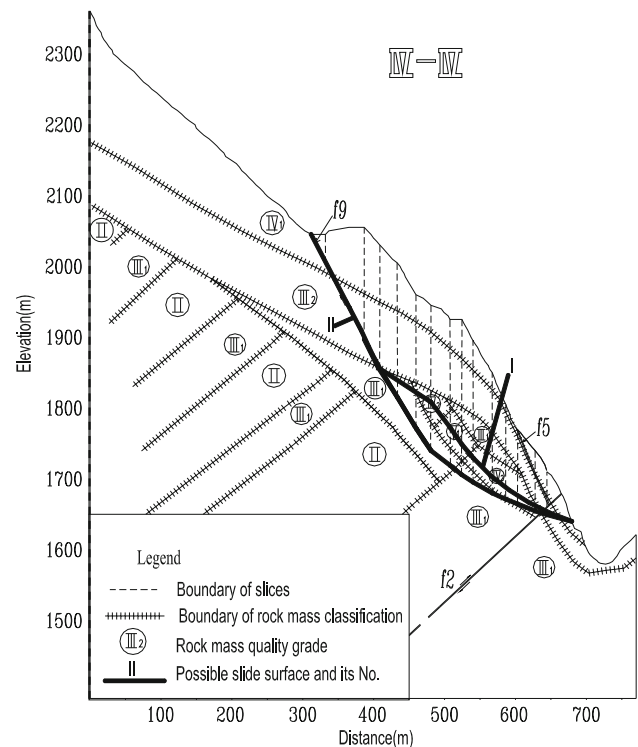
Table 2 Parameters of rock mass and discontinuities used in stability analysis

Rock property	Density (kg/m³)	Rock mass grade	Cohension, C (MPa)	Friction angle, φ (°)	Tension strength, σ_t (MPa)	Deformation modulus, E (GPa)	Possion ratio, v
Marble	2750	II	2.00	53.47	8.43	23.5	0.225
		III$_1$	1.50	46.94	8.43	10.5	0.25
		III$_2$	0.90	45.57	4.69	5.5	0.275
		IV$_1$	0.60	34.99	0.60	2.5	0.3
		IV$_2$	0.40	30.96	0.40	1.9	0.3
Sandy slate	2720	II	2.00	53.47	8.43	23.5	0.225
		III$_1$	1.50	46.94	8.43	10.5	0.25
Fault	2,780	IV$_1$	0.60	34.99	0.60	2.5	0.3
		V$_1$	0.02	16.7	0	0.4	0.35

Type	Characteristics	Representative discontinuities	Cohension, C (MPa)	Friction angle, φ (°)
Fresh rigid joint	Planar, slight roughness, slightly-weakly weathered, without cement, moderate strength	Fresh rigid joints dipping outward and located in the weakly unloading zone (set ② joints)	0.00	26.1
Fault zone	The surface is planar and smooth, bearing mud locally, the zone mainly consists of lithic fragments and fine-moderate breccias, with a lithic fragment content of 15–25% and breccias of 60–80%	f_5, f_8, f_9, f_2, and some deep cracks i.e. SL24, SL15	0.02	14.0
	Planar and rough, open, bearing mud film or filled with mud locally, without cement	Some deep cracks i.e. SL20, SL22, SL23, SL47, SL48, SL43	0.00	19.3
	Undulated planar, slight roughness, long extension, open and without fill	Some deep cracks i.e. and large unloading cracks i.e. SL13, SL14, SL18, SL19, SL21(SL42)	0.00	16.0

Results and analysis

Figures 10 and 11 show the rock slice cross sections which have been analysed. The results, using the Sarma method, indicate that at section VI-VI the slope had a FOS of 1.026 along slide surface I and at IV-IV a FOS of 1.053, again along slide surface I (Table 1).

In order to better understand the influence of the deep cracks in the left slope for the global stability, in addition to the Sarma method, the strength reduction method based on FLAC^{3D} was adopted as this does not require an assumption to be made in advance about the shape or location of the failure surface. It can be seen from Fig. 12a that the critical surface of section VI-VI is along f_5 which has a corresponding FOS of 0.95. Figure 12b indicates that the critical surface of section IV-IV, which includes fault f_9 and SL22–SL24, the corresponding FOS is 1.05.

The results of slope stability obtained by the strength reduction method are similar to those obtained by the Sarma method. Furthermore, it can be seen from the results

of the plastic zone distribution (Fig. 12) that the deep-seated cracks play a significant role in the location of the slide surface in sections VI-VI and IV-IV, as the inferred shear failure zones in both sections potentially indicate a high concentration of stress with a similar attitude and distribution as the deep cracks.

The calculations indicate that the left bank slope is not mathematically stable and to ensure its safety some remedial works will be necessary.

Remedial works

To improve the stability of the left slope where the deep cracks are present, anchoring would not be practical in view of the distance in from the valley side. As a consequence cement infilling of special galleries and grouting was adopted to improve the quality of the rock mass. Three places with deep cracks (SL1, SL2 and SL3—see Fig. 5c) were chosen to check the effectiveness of the grouting
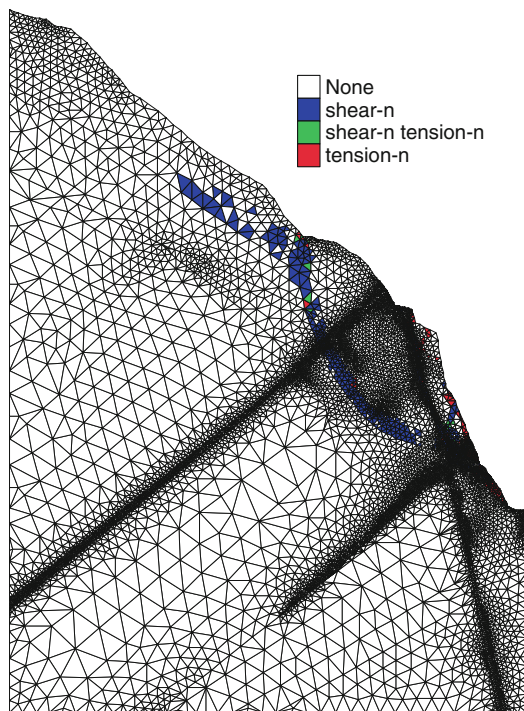
(a)
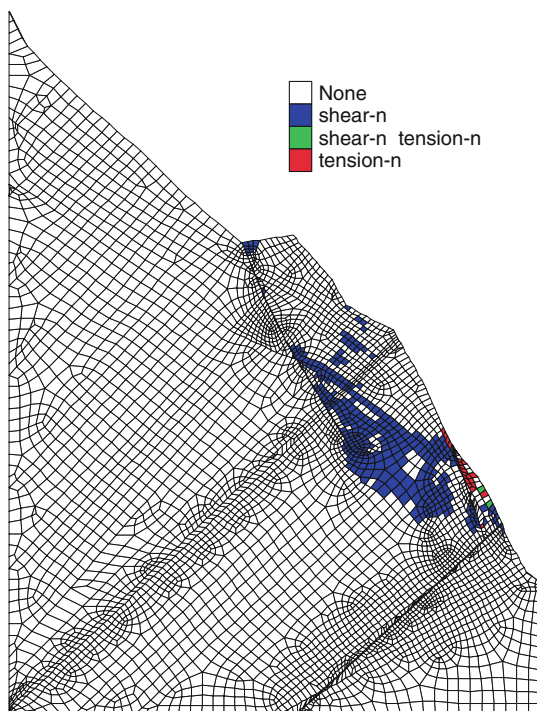
(b)

Fig. 12 The result reached by strength analysis based on FLAC^{3D}. **a** Cross section VI-VI. **b** Cross section IV-IV

method, the deformation modulus, acoustic wave velocity and permeability ratio of the rock mass after grouting (see Table 3).

Table 3 Some parameters of rock mass with deep cracks before and after grouting

	Permeability (Lu)			Acoustic wave velocity (m/s)			Borehole deformation modulus (GPa)	
	Max.	Min.	Mean	Max.	Min.	Mean	Range	Mean
Pre-grouting	93.00	12.00	52.50	4,386	1,506	2,750	1.78–3.68	2.65
Post-grouting	2.22	0.58	1.12	5,000	1,701	3,830	3.20–6.62	4.96

Table 3 indicates that the pre-grouted rock mass has moderate permeability (10–90 Lugeons) while after grouting the rock mass was only slightly permeable (0.6–2.0 Lugeons). Single hole and cross hole acoustic measurements indicate that the mean acoustic wave velocity of the rock mass before grouting was 2,750 m/s and increased to 3,830 m/s after grouting. Borehole deformation modulus tests show that grouting can increase the mean deformation modulus of the rock mass by a factor of approximately 1.9, compared to the value of 2.65 GPa before grouting (see Table 3).

All these results demonstrate that the quality of the rock mass with deep cracks is dramatically improved after grouting, hence it is reasonable to assume that the shear strength properties of the grouted rock mass were also improved. As a consequence it was decided that the excavation of tunnels to be infilled with grouting would be an effective way of enhancing the stability of the slope.

Conclusions

This paper discusses the deep seated cracks/crack zones encountered in the rock mass on the left side of the valley where the dam for Jinping I hydropower station will be constructed. The deep seated discontinuities were originally tectonic discontinuities (i.e. joints and faults). The rock mass in which these major cracks occur have a low acoustic wave velocity, are fractured, have a high permeability and abnormally low ground stress. The RMR and Q systems indicated a very poor rock mass which was further weakened by the presence of the deep cracks, implying an only marginally stable slope.

Two typical sections of the slope were evaluated using the Sarma and strength reduction methods. The results demonstrate that the spatial distribution of the deep cracks plays a significant role in the potential failure mechanism. As a consequence, the slope cannot be considered safe and hence some remedial works are necessary. In view of the horizontal distance from the free face, the grouting of specially constructed tunnels was recommended. Some typical in situ tests results indicate that the quality of rock

mass with the deep cracks can be significantly improved by such grouted galleries.

References

Barton N, Lien R, Lunde J (1974) Engineering classification of rock masses for the design of tunnel support. Rock Mech 6:183–236

Bieniawski ZK (1979) The geomechanics classification in rock engineering applications. In: Proceedings of 4th Int Congr Rock Mech, vol 2. ISRM, Montreux, pp 41–48

Burchfiel BC, Stewart JH (1966) "Pull-apart" origin of the central segment of Death Valley, California. Geol Soc Am Bull 77:439–442

CBPRC (Construction Bureau of People's Republic of China) (1994) Chinese Code of Engineering Rock Mass Classification (GB 50218-94), PP4 & PP7

Griffiths DV, Lane PA (1999) Slope stability analysis by finite elements. Geotechnique 49(3):387–403

Institute of Chengdu Investigation and Design of National Electrical Power (2001) Report of selecting dam site for Jinping first stage hydropower station, 4 Engineering geological condition (In Chinese)

Institute of Chengdu Investigation and Design of National Electrical Power (2002) Engineering Geology Report of concretion grout test on relaxed and cracked rock mass at the left slope in the dam site of Jinping I Hydropower Station (In Chinese)

Qi S, Wu F, Yan F, Lan H (2004) Mechanism of deep cracks in the left bank slope of Jinping first stage hydropower station. Eng Geol 73(1–2):129–144

Sarma SK (1979) Response and stability of earth dams during strong earthquakes. Waterways Experiment Station, Vicksburg, Paper GL-79-13

Wu S, Shen M, Wang J (2010) Jinping hydropower project and main technical issues on engineering geology and rock mechanics. Bull Eng Geol Environ. doi:10.1007/s10064-010-0272-4